Epidemics 7 (2014) 13–21

Contents lists available at ScienceDirect

Epidemics

journal homepage: www.elsevier.com/locate/epidemics

Modelling the effect of changes in vaccine effectiveness and transmission contact rates on pertussis epidemiology

P. Pesco [a], P. Bergero [a], G. Fabricius [a,*], D. Hozbor [b]

[a] Instituto de Investigaciones Fisicoquímicas Teóricas y Aplicadas, Facultad de Ciencias Exactas, Universidad Nacional de La Plata, CC 16, Suc. 4, 1900 La Plata, Argentina
[b] Laboratorio VacSal. Instituto de Biotecnología y Biología Molecular, Departamento de Ciencias Biológicas, Facultad de Ciencias Exactas, Universidad Nacional de La Plata y CCT-La Plata, CONICET, Calles 47 y 115, 1900 La Plata, Argentina

ARTICLE INFO

Article history:
Received 4 September 2013
Received in revised form 10 March 2014
Accepted 3 April 2014
Available online 13 April 2014

Keywords:
Pertussis
Transmission
Mathematical model
Outbreaks
Epidemiological trends

ABSTRACT

The incidence of the highly infectious respiratory disease named pertussis or whooping cough has been increasing for the past two decades in different countries, as in much of the highly vaccinated world. A decrease in vaccine effectiveness over time, especially when acellular vaccines were used for primary doses and boosters, and pathogen adaptation to the immunity conferred by vaccines have been proposed as possible causes of the resurgence. The contributions of these factors are not expected to be the same in different communities, and this could lead to different epidemiological trends. In fact, differences in the magnitude and dynamics of pertussis outbreaks as well as in the distribution of notified cases by age have been reported in various regions.

Using an age-structured mathematical model designed by us, we evaluated how the changes in some of the parameters that could be related to the above proposed causes of disease resurgence – vaccine effectiveness and effective transmission rates – may impact on pertussis transmission.

When a linear decrease in vaccine effectiveness (VE) was assayed, a sustained increase in pertussis incidence was detected mainly in infants and children. On the other hand, when changes in effective transmission rates (β_{ij}) were made, a dynamic effect evidenced by the presence of large peaks followed by deep valleys was detected. In this case, greater incidence in adolescents than in children was observed. These different trends in the disease dynamics due to modifications in VE or β_{ij} were verified in 18 possible scenarios that represent different epidemiological situations. Interestingly we found that both incidence trends produced by the model and their age distribution resemble the profiles obtained from data reported in several regions. The implications of these correlations are discussed.

Introduction

After the introduction of vaccination programs, the morbidity and mortality associated with the respiratory disease called pertussis or whooping cough decreased substantially. However, pertussis-related hospital admissions and fatalities are still evident, particularly in young infants. Most reported deaths occur in unvaccinated or incompletely vaccinated infants who are younger than 12 months. Nevertheless, the disease also affects adolescents and adults (de Melker et al., 2006).

During the last two years large outbreaks have been detected in Australia, the Netherlands, the UK and the US (Spokes et al., 2010; DeBolt et al., 2012; Public Health, 2013; Winter et al., 2012). The possible causes for this disease outbreaks and resurgence are still under debate and include a decrease in vaccine effectiveness over time (waning immunity) and pathogen adaptation (Mooi, 2010; Klein et al., 2012; Misegades et al., 2012; Sheridan et al., 2012).

Since pertussis vaccination is the best strategy to control pertussis disease cases, it is possible to suspect that some of the recent epidemiological features could be the consequence of failures in current vaccine effectiveness. In fact, there is recent evidence showing that acellular vaccines (aP) induce protection for less time than the whole-cell vaccines (wP) (McCarthy, 2013). Acellular vaccines were developed because of concerns that the whole-cell vaccines caused neurological and other reactions in children. Because of such concerns in the 1980s and 1990s wP vaccines were gradually replaced with aP in some countries. As an example of the failure of acellular vaccines, in a case–control study designed to assess the risk of pertussis among 10–17 year olds during the 2010–2011 outbreak in northern California, the researchers found that teenagers

* Corresponding author. Tel.: +54 2214257430; fax: +54 2214254642.
E-mail address: fabricius@fisica.unlp.edu.ar (G. Fabricius).

http://dx.doi.org/10.1016/j.epidem.2014.04.001

who had received four whole-cell vaccines were nearly six times less likely to have been given a diagnosis of pertussis than those who had received all acellular vaccines and nearly four times less likely than those who had received a mix of vaccines (Klein et al., 2013). It is proposed that the switch to the acellular vaccine may partly explain the resurgence of pertussis. Beyond the fact that the effectiveness of the vaccines may be reduced by the change from cellular to acellular vaccines, it can also be altered by the divergence between circulating bacterial strains and those used in vaccine production. It was proposed that the selection pressure exerted by vaccines has selected circulating bacteria. It is expected that the predominance of a particular geno/phenotypic bacterial background is not the same everywhere because of the different formulations and vaccination schemes used (i.e prn minus strains, see below).

Regarding pathogen adaptation, antigenic divergence detected initially involved mutations affecting the *B. pertussis* proteins included in the acellular vaccines. This divergence could affect pertussis transmissibility. In the 1990s, strains emerged with a novel allele for the Ptx promoter, ptxP3 strains produce more Ptx in vitro (Mooi et al., 2009). The ptxP3 strains have risen to predominance replacing the resident ptxP1 strains in many European countries, the US and Australia (Mooi et al., 2009; Advani et al., 2011; Lam et al., 2012; Petersen et al., 2012; Schmidtke et al., 2012) and also in Argentina. Van Gent et al. reported that the detected variation in the promoter for pertussis toxin (ptxP) and Prn contribute significantly to differences in colonization (van Gent et al., 2011). Regarding pertactin, the analysis of a subset of strains with the same ptxP allele revealed that the ability to colonize mice increased in the order Prn1 < Prn2 and Prn3. The increased colonization of strains containing Prn2 could also involve greater transmissibility.

More recently, strains that do not express one or more components of pertussis vaccines, in particular Prn, have emerged (Barkoff et al., 2012; Hegerle et al., 2012; Otsuka et al., 2012). In particular in US it was reported that pertactin-deficient isolates increased substantially over 50% in 2012 (Pawloski et al., 2014). PRN is a surface protein, which contains a RGD motif (Arg-Gly-Asp) involved in the attachment of *B. pertussis* to mammalian cells. Using animal (mice) models it was observed that PRN-deficient isolates are able to multiply in the respiratory tract of young mice but not in the respiratory tract of adult mice, suggesting a decrease in virulence in adults (Bouchez et al., 2009). Taking into account these results and the known role of pertactin as an adhesin, it is possible to suggest that this deficiency in protein that in principle helps the bacteria to subvert the immune response conferred by vaccines, especially those of the acellular vaccine, would also have an impact on pertussis transmission. Thus, an infectious individual carrying a pertactin-negative isolate may lead to a lower infective contact than that produced by an individual carrying a pertactin-positive isolate. At this point it is important to note that the effective contact can be modified differently depending on which geno-phenotype of bacteria in bacterial population prevails: if strains not expressing pertactin prevail, the contact rate decreases; whereas if Prn2 strains prevail, colonization increases and transmission might be greater.

Moreover, effective contact rates can be affected by other factors independent of pathogen adaptation, e.g., use of acellular vaccines. It has recently been demonstrated in a non-human animal model that acellular vaccines fail to prevent colonization and transmission, increasing the infectivity of contact rates (β_{ij})(Warfel et al., 2014). Another reason that may produce a global change in β_{ij} is a health campaign conducted against pertussis or other diseases that indirectly affect pertussis transmission (i.e., during pandemic flu). This could cause a transient reduction of β_{ij}, assuming that health care is strong for a limited period of time, usually when public health problems are very evident, and then, when the risks decrease the population becomes more relaxed in the implementation of such health cares.

All the aforementioned data show the relevance of analyzing the effect of changes in vaccine effectiveness and transmission contact rates on pertussis epidemiology.

In this work we use our previously designed mathematical model for pertussis transmission to evaluate possible changes in the effectiveness of the vaccine and in β_{ij} in 18 different possible epidemiological scenarios. These scenarios consider different contact patterns among individuals, different duration of natural or vaccine-induced immunity and different vaccination coverage. With our model we observed that the impact on pertussis epidemiological profile caused by the change in the effectiveness of the vaccine differs from that produced by global changes in β_{ij}. Beyond the intrinsic relevance of our findings, interestingly we could correlate our results with epidemiological profiles obtained from data reported in different regions.

Materials and methods

In this work we used our previously designed age-structured compartmental model with 9 epidemiological classes (Fabricius et al., 2013). The schema of the model is presented in Fig. 1. The 9 epidemiological classes shown in the figure are divided into 30 age groups. Thus, for fully susceptible individuals, for example, we define $S_i(t)$ as the fraction of individuals in class S, at time t, with age in the interval (a_i, a_{i+1}). The force of infection λ_i is the rate at which susceptible or partially immune individuals of age group i acquire infection. This is the only rate in our model that is not constant through time and depends on the fractions of infected individuals (which are dynamical variables of the model) through the expression:

$$\lambda_i = \sum_j \beta_{ij} I_j^* \quad ; \quad I_j^* = I_{1j} + \rho_1 I_{2j} + \rho_2 I_{3j} \tag{1}$$

where β_{ij} is the contact parameter matrix and I_j^* is the effective fraction of individuals of age j in the population that is infective. Factors ρ_1 and ρ_2 are taken smaller than one to consider that infected individuals in classes I_2 and I_3 are less infective than the ones in I_1 class

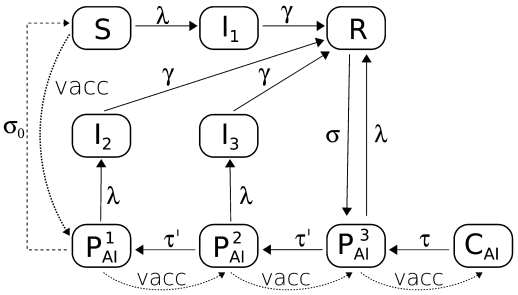

Fig. 1. Schematic representation of the mathematical model. Individuals are in the susceptible epidemiological class S when born, and remain there except when they become infectious through contact with an infected individual and enter the full symptomatic infective class I_1, or they acquire the lowest level of immunity through the first vaccine dose and enter P^1_{AI} (P_{AI}: Partial Acquired Immunity). When receiving successive vaccination doses (dotted lines), individuals go through classes of increasing immunity and eventually reach the C_{AI} (Complete Acquired Immunity) class. Individuals in classes P^1_{AI} and P^2_{AI} develop a less symptomatic illness when they get infectious, entering class I_2 (mild infection) or I_3 (weak infection), respectively. In this model, infection fades in a time $1/\gamma$. After this time, individuals in infective classes I_1, I_2 or I_3 recover and enter class R. Individuals in P^3_{AI} class acquire an extremely weak infection, thus they do not become infective and directly enter R class. Individuals in partial or complete immunity classes decrease in their immunity levels at rates σ, τ and τ' and they eventually become completely susceptible at a very slow rate τ_0.

For details see ref. (Fabricius et al., 2013).

as they have a milder cough. To assign the parameter values of the model, due to the uncertainties in some of them, different epidemiological scenarios including different contact patterns among individuals, different duration of natural or vaccine-induced immunity and different vaccination coverage were considered. Each one of the 18 scenarios considered represents, in principle, a possible description of pertussis transmission. In this way, with our model we are able to check which results are robust and which ones depend on a particular choice of parameters. A detailed description of the model and the parametrization scheme are presented in the Supplementary Data and in Ref. (Fabricius et al., 2013). In this study we first present the results obtained with the scenario CP_{1A}-MDI-C_{95}. This scenario includes the contact rate parameters β_{ij} obtained from forces of infection in pre-vaccine era, intermediate values reported for the duration of pertussis immunity and vaccination coverages of 95% for the first dose.

To evaluate the impact of changes in vaccine effectiveness and transmission contact rates on pertussis epidemiology, we started in the stationary state of our model and introduced a perturbation of the system transferring 25% of individuals from Susceptible (S) to Recovered (R) classes. By performing this perturbation we mimicked the typical periodicity of pertussis outbreaks. This is a common practice when using deterministic models (Rohani et al., 2002) to obtain the oscillations that any stochastic consideration would anyway introduce. After the disturbance, the system is allowed to evolve for 20 years and then we introduce the following parameter changes: (I) a linear reduction in vaccine effectiveness (VE), (IIa) a linear reduction in the effective contact rate parameters β_{ij}, (IIb) a linear increase of β_{ij} and (IIc) a linear reduction in β_{ij} followed by a linear increase in the original values (hereafter referred to as transient reduction).

In the first case, the linear reduction in vaccine effectiveness is performed over a period $t_{VE} = 12$ years in order to obtain the arbitrary value of 40% of protected population at the end of the period. For the initial value we considered $VE_i = 0.9$ for the first 5 doses (Hethcote, 1997) and $VE_i = 0.5$ for the Tdap adolescent booster. After the period t_{VE} the vaccine efficacy of all doses was multiplied by 0.53, so, the vaccine efficacy for the primary dose was changed to $VE_f = 0.48$ at the end of the period (for details see Supplementary Data). Other values for VE_f and t_{VE} were also considered in order to study the dependence of our results on these parameters (Supplementary Data).

In the second case, each linear increase or reduction in the effective contact rate parameters β_{ij} is performed over a time $t_\beta = 2$ years and has a magnitude of 20%. Then, at the beginning of the perturbation $\beta_{ij} = \beta_{ij}^{(0)}$ for the three situations, but at the end $\beta_{ij} = 0.8\beta_{ij}^{(0)}$ in case (IIa), $\beta_{ij} = 1.2\beta_{ij}^{(0)}$ in case (IIb), and $\beta_{ij} = \beta_{ij}^{(0)}$ in case (IIc). In this case, simulations with different values of t_β were also performed.

The effects of these parameter changes on pertussis transmission are studied analyzing the evolution of the dynamic variables of the model obtained through numerical resolution of a system of coupled differential equations (Supplementary Data). In particular, we focused our attention on pertussis incidences of fully (Inc_1) and mild (Inc_2) symptomatic pertussis cases, which are the most risky classes. These incidences may be computed for each one of the 30 age groups as follows:

$$Inc_{1i} = \lambda_i S_i, \quad Inc_{2i} = \lambda_i P^1_{AI_i}$$

where S_i and $P^1_{AI_i}$ are the fractions of individuals of age group i in classes S and P^1_{AI} (P_{AI}: Partial acquired immunity), respectively, and λ_i is the force of infection. In this work we evaluate the dynamic evolution of the sum $Inc_i(t) = Inc_{1i}(t) + Inc_{2i}(t)$ of both fully and mild pertussis cases. We also evaluated the age distribution of incidence at fixed times.

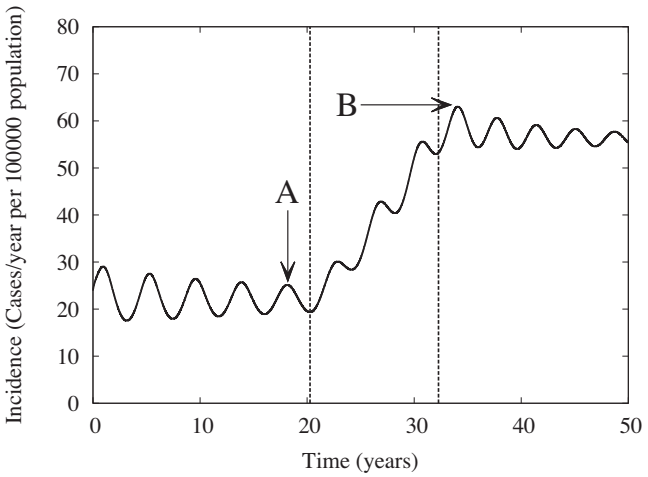

Fig. 2. Dynamic evolution of pertussis incidence of infants (0–1 year) when vaccine effectiveness is reduced. VE was linearly varied from $VE_i = 0.9$ to $VE_f = 0.48$ over a period $t_{VE} = 12$ years. Peaks A and B correspond to the maximum of incidence before and after the change in VE was introduced. The dotted lines indicate the start and finish times of the VE change.

Results and discussion

Change in vaccine effectiveness

In our model the changes in pertussis vaccine effectiveness can be introduced by changing the fraction of the population that is transferred to a class of higher immunity after each dose application. The magnitude of the changes in vaccine effectiveness and the period of time during which they take place are variables to be considered. Fig. 2 shows the temporal evolution of incidence in 0–1y age group when VE is reduced by a factor 0.53 for all vaccine doses over a period of 12 years. The reduction in vaccine effectiveness induces a gradual increase of incidence that leads to a new stationary state with an incidence 2.5 times higher than the original value of 22.3 cases per 100,000 inhabitants per year. The same behavior was observed for the incidences of pertussis disease in 0–15y age group (not shown) – with an incidence 1.7 times higher in the new stationary state. The total incidence (all age groups), however, presents a lower increase of 27%, highlighting that the reduction in vaccine effectiveness essentially affects infants and children. As is expected, the magnitude of the increase in pertussis incidence depends on the reduction in the VE parameter (Fig. S1 of Supplementary Data) reaching incidence values that correspond to pre-vaccine era when VE = 0.

A reduction in the period of time in which vaccine effectiveness is modified increases the incidence value of peak B of Fig. 2, which then approaches the endemic state (Fig.S2 of Supplementary Data).

Change in disease transmissibility

We considered next possible changes in the effective contact rate parameters β_{ij} and analyzed their impact on pertussis transmission.

We first focused our attention on the effect that a decrease in β_{ij} could produce. To this end, we linearly reduced arbitrary the values of all β_{ij} to 80% of their initial values in a period of 2 years (case IIa). In this case, the 0–1y incidence profile presents sharp and high peaks falling down to very low values after each peak (Fig. 3a). The incidence oscillates slowly approaching a new stationary state that has a value only 12% lower than that before the perturbation was introduced.

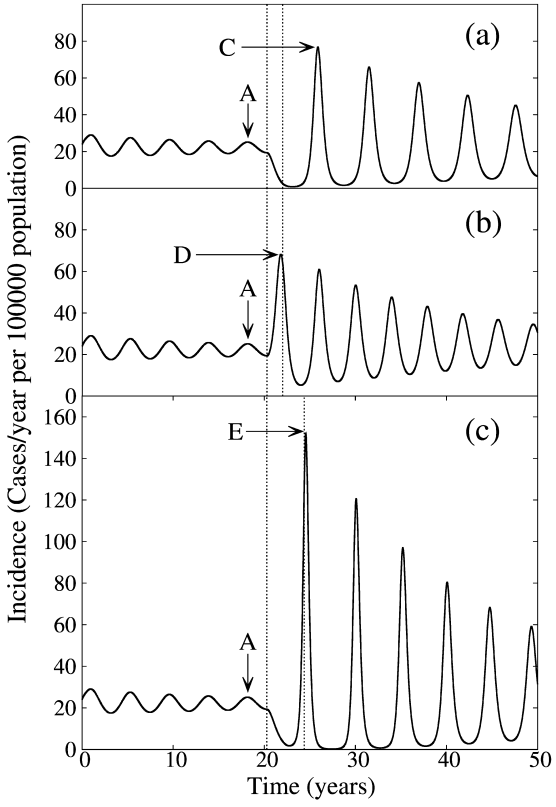

Fig. 3. Dynamic evolution of pertussis incidences of infants (0–1 year) when disease transmissibility is modified. The dotted lines indicate the start and finish times of the changes in parameters. In panel (a), β_{ij} parameter values were linearly reduced a 20% of the initial values over a period $t_\beta = 2$ years. Peaks A and C correspond to the maximum of incidence before and after the change in β_{ij} was introduced. In panel (b), β_{ij} parameter values were linearly increased a 20% of the initial values over a period $t_\beta = 2$ years. Peaks A and D correspond to the maximum of incidence before and after the change in β_{ij} was introduced. In panel (c), β_{ij} parameter values were linearly reduced a 20% of the initial values over $t_\beta = 2$ years and then recovered the original values over the 2 following years (transient reduction). Peaks A and E correspond to the maximum of incidence before and after the change in β_{ij} was introduced.

We also evaluated what happens when β_{ij} are linearly increased by 20% from their initial values over a period of 2 years (case IIb). Fig. 3b shows the temporal evolution of pertussis incidence in 0–1y age group. In this case, the dynamic behavior of 0–1y incidence is similar to that of case (IIa), but with less pronounced maxima and minima. However, there is not a deep minimum after the introduction of the perturbation as in the above case, and the stationary value of incidence increased by 8%. Finally, in Fig. 3c we show the 0–1y incidence for case IIc, where β_{ij} were reduced transiently. In this case, the 0–1y incidence presents a similar dynamic behavior to that of the other cases but the peaks and minima are even more pronounced than in cases IIa and IIb approaching the original value of incidence very slowly (as expected, as the final parameter values are unchanged at the end of the perturbation).

For other age groups, the incidence calculated with our model shows the same dynamic behavior as the one of 0–1y age group (Fig. 3) with incidence values for the stationary state around or less than 10% of the initial values, previous to the perturbation.

In contrast to the effect produced by the reduction in vaccine effectiveness (the system reaches a stationary state of higher incidence), changes in the contact parameter rates cause a pronounced difference between the maxima and minima, which is much greater than the slight change in the stationary value of incidence, if any. Moreover, in case (IIc), immediately after β_{ij} reach their original values, the mean value of incidences over a period of oscillations is equal to that found before introducing changes in β_{ij} values (Fig. S3 from Supplementary Data). The changes in β_{ij} lead to a transient change in the stationary values of S_i and $P_{\mathrm{AI}i}$ (fraction of individuals of S and P_{AI} classes) that triggers a dynamic effect. The pronounced oscillations observed in the incidence values are a consequence of such dynamic effect. This could be better understood using a simple SIR model that has only 1 class of susceptible and infectious individuals (See Appendix for an explanation of this effect). The fact that the dynamic effect is already present in the simple SIR model shows that this behavior is not a consequence of the complexity of the model, but is produced by the global change in β_{ij}.

If the change in β_{ij} occurs much more slowly, the height of peaks will be drastically reduced and the effect will be less noticeable. (See Supplementary Data, Fig. S4, for details).

It is important to note that all the conclusions obtained here remain independently of the epidemiological state of the system when perturbations were introduced (i.e., the incidence is at a maximum, minimum, increasing, or decreasing, Fig. S5a and b, Supplementary Data).

It is noticeable that in all cases considered, a reduction in vaccine effectiveness does not lead to dynamic behavior included in Fig. 3. Even though very low values were taken for VE, in none of the cases analyzed the model predicts the pronounced minima of incidence observed when transmissibility parameters are changed.

Specific Age Incidences (SAI)

The specific age incidence in age interval Δ at time t is defined as $(\mathrm{Inc}_1(t) + \mathrm{Inc}_2(t))/\Delta$, where Inc_1 (Inc_2) are the sum of Inc_{1i} (Inc_{2i}) for all the age groups contained in Δ. We computed SAI to observe the age distribution of incidence at the outbreaks before and after the described changes in parameters were introduced. In Fig. 4, the SAI values at peaks A and B are shown. These peaks correspond to the maximum of incidence observed before and after the reduction in vaccine effectiveness was introduced (Fig. 2). The SAI values in B are increased in relation to those of A mainly in infants and children, the relative increment being higher in infants. This result is expected since this age group is directly protected by vaccination and consequently will be more affected when vaccine effectiveness is reduced. In Fig. 5 the SAI values at peaks A and E are shown. These peaks correspond to the maximum of incidence before and after the effective contact rate parameters β_{ij} were changed for case IIc (Fig. 3c) where there is no change in

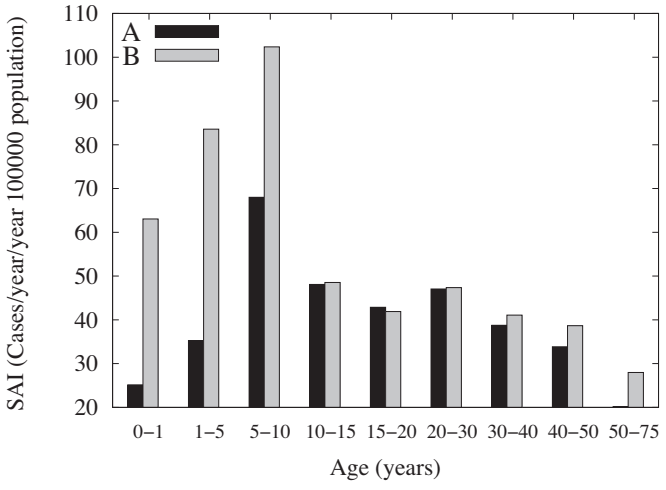

Fig. 4. Variation of specific age incidence (SAI) as a consequence of a reduction in vaccine effectiveness. SAI values calculated at peak A (before VE change was introduced) of Fig. 2 and peak B (after VE change was Introduced) of Fig. 2.

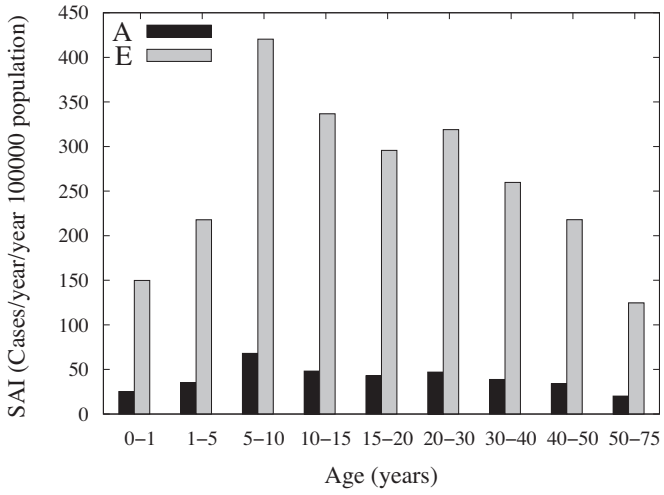

Fig. 5. Variation of specific age incidence (SAI) as a consequence of a transient reduction of disease transmissibility. SAI values calculated at peak A (before β_{ij} change was introduced) of Fig. 3c and peak E (after β_{ij} change was Introduced) of Fig. 3c.

the stationary value of incidences. The changes in SAI values from peak E to A (Fig. 5) are higher than those of B to A (Fig. 4). The age distribution of incidence is very similar before (peak A) and after (peak E) β_{ij} change, indicating that the dynamic effect that caused the high incidence peaks does not essentially modify the age profile of SAI. Comparisons of SAI values of infants with those of teenagers are presented in Table 1. When vaccine effectiveness is reduced, the SAI values in infants and young children (0–5y) are greater than those of teenagers (10–15y). Otherwise, at peak E (Fig. 3c), after β_{ij} have been modified and returned to their original values, SAI values in teenagers are greater than in infants. In Table 1 f = SAI(0–5y)/SAI(10–15y) is also presented to quantify the relation between incidences of both age groups in the different situations analyzed. We have also included the quotient for cases IIa and IIb, where the stationary values of incidence slightly change with respect to peak A (previous to the introduction of changes). In these cases the quotient is also smaller than 1 showing that SAI in adolescents is higher than in infants as in case IIc.

To check the robustness of these results and their possible dependence on local epidemiological features, we repeated the calculations for the 18 scenarios we have previously described (Fabricius et al., 2013). Interestingly, the qualitative results discussed remain valid for all the scenarios analyzed. In particular, SAI in infants is always larger than in teenagers ($f > 1$) when vaccine effectiveness is reduced and the opposite holds ($f < 1$) when effective rate transmission parameters are changed (see Table S5 in Supplementary Data). The numerical value of the f-quotient changes for different scenarios giving an estimation of the sensibility of the predicted value to uncertainties in the parameters. We have also checked that the value of f-quotient is little influenced by the efficacy of the Tdap adolescent booster (see Table S6 in Supplementary Data).

Summary of our model simulations

In summary, our results show that when vaccine effectiveness was reduced, the disease incidence (mainly in infants) increased with periodic outbreaks towards a new stationary value. The increase of infant incidence inverted the relation Inc(0–5y) < Inc(10–15y) characteristic of vaccine era (Fabricius et al., 2013; Hethcote, 1997; Luz et al., 2006). When transmission rate parameters β_{ij} were reduced, the model predicted a basically dynamic effect that produced very high peaks followed by deep valleys with a slight modification of the stationary values of incidence. When β_{ij} were reduced transiently (and there was no change of the final stationary state of the system) the dynamic effect was even more pronounced. In any case, when β_{ij} were modified, the relation of incidences Inc(0–5y) < Inc(10–15y) characteristic of vaccine era was preserved.

These results were obtained changing parameters VE and β_{ij} independently of each other in order to analyze the effects that each may cause on pertussis transmission. The results obtained were verified in 18 different scenarios that represent possible epidemiological situations, indicating that the epidemiological trends predicted by the model are robust. However, it is important to note that the profiles obtained from epidemiological reports may result from a sum of the effects considered (and others) in which the weight of each one can vary from place to place, from population to population.

Epidemiological trends in different US states and their comparison with the incidence profiles obtained with the model

We analyzed data reported by one of the countries (US) where pertussis resurgence is evident and molecular epidemiology and microbiology databases are accessible. Interestingly, we noticed that though the reported cases in the whole country increased steadily until 2013, the epidemiological profiles during 1993–2013 differ among the states. However, it is remarkable that some profiles are similar for various states (Fig. 6) and they are also similar to the profiles from the model when VE is reduced (Fig. 2). Furthermore, other states have similar profiles (Fig. 7) and they bear a close resemblance to the ones from the model when β_{ij} are diminished permanently o transiently (Fig. 3a and c). Fig. 6 shows the data reported for the states of Texas, Ohio and Alabama, and Fig. 7 the data corresponding to Wisconsin, Montana and Washington. These figures show that the states included in Fig. 6 have profiles with an increasing trend in the incidence, while the states included in Fig. 7 present very sharp peaks with very few cases before and between the peaks. In the case of Washington there is just a single peak in 2012 but, before and after the peak, the reported cases diminish drastically as occurs in Wisconsin and Montana. For all

Table 1
Specific age incidences (SAI) in children and adolescents before and after changes in vaccine effectiveness (VE) or transmission parameters β_{ij} were introduced. Quotient f between SAI in children and teenagers is also given.

	SAI (0–5y)	SAI(10-15y)	f = SAI(0–5y)/SAI (10–15y)
Peak A (Figs. 2 and 3) Previous to the introduction of parameter changes	33.2	48.0	0.69
Peak B (Fig. 2) After change in VE was introduced	79.5	48.6	1.64
Peak C (Fig. 3a)	115.3	239.0	0.48
Peak D (Fig. 3b)	80.9	104.9	0.77
Peak E (Fig. 3c) After global changes in β_{ij} were introduced	204.2	336.6	0.61

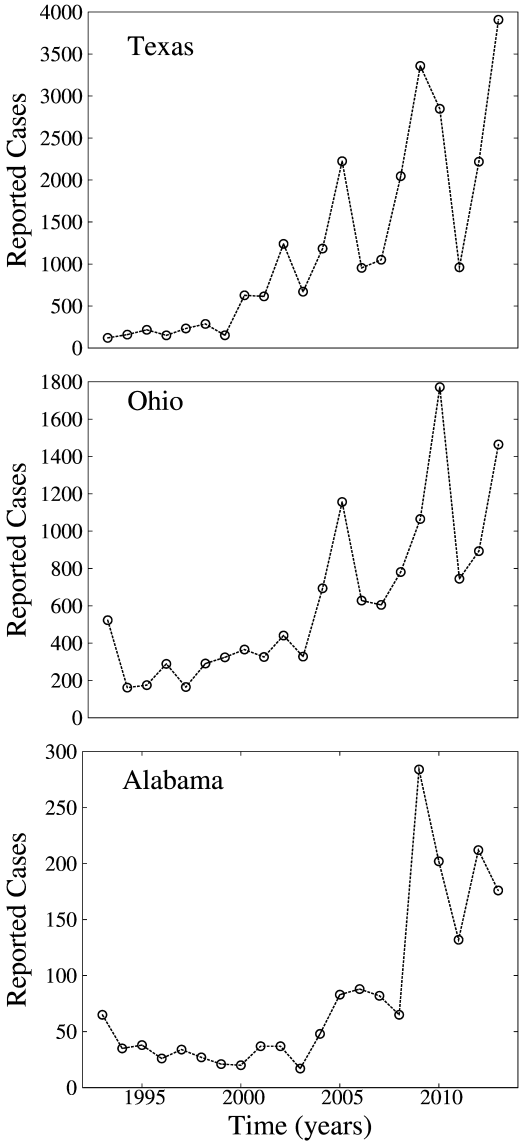

Fig. 6. Reported cases per year for Texas, Ohio and Alabama in the period 1993–2013.
Data from ref. (Texas, 2013a) for Texas and ref. (CDC, 2014) for Ohio and Alabama.

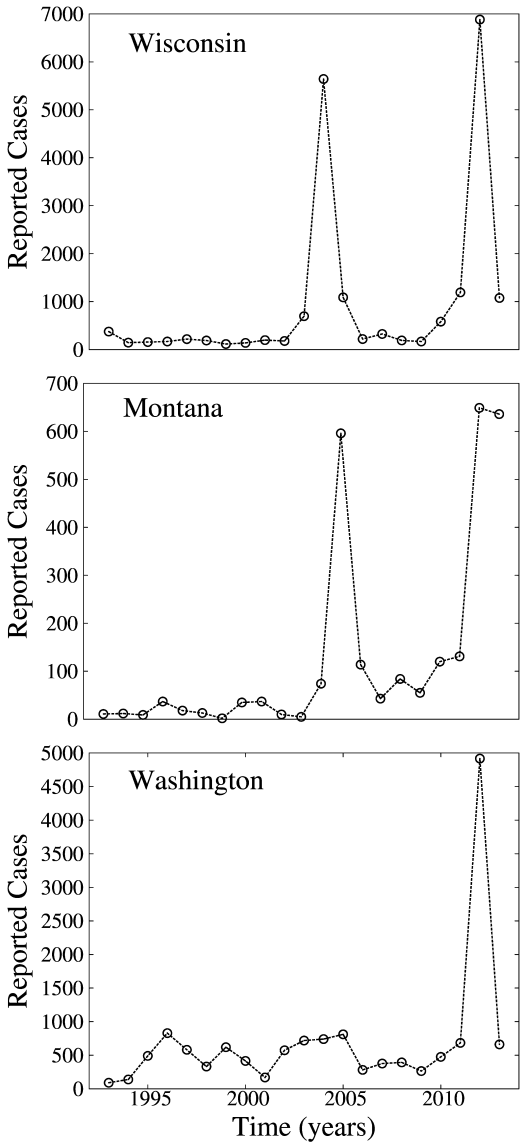

Fig. 7. Reported cases per year for Wisconsin, Montana and Washington in the period 1993–2013.
Data from ref. (CDC, 2014).

these states we evaluated the proportion of cases in children and adolescents at the peak. In particular, we analyzed the quotient f_R of reported cases in the 0–5y and 10–15y age groups for each state analyzed (Table 2). In Table 2 we can observe that the estimation of f_R is greater than 1 when it is computed for the peaks corresponding to Fig. 6 and it is lower than 1 when the computation is performed for the peaks of Fig. 7.

Table 2
Estimation of the ratio f_R of reported cases in children (0–5y) and teenagers (10–15y) for selected States of USA. The quotient was performed for the highest peak. In the states where the distribution of cases by age was not available for the considered age range, linear extrapolations were performed.

State	Peak	Source of data	f_R
Texas	2009	Texas (2013b)	2.21
Ohio	2010	Ohio (2010)	1.18
Alabama	2009	Alabama (2009)	2.93
Wisconsin	2012	Wisconsin (2013)	0.5
Washington	2012	Washington (2013)	0.86
Montana	2012	Montana (2012)	0.79

Comparing the results obtained in Tables 1 and 2, we may conclude that when incidences present a sustained increase in time (Figs. 2 and 6) it is observed at the outbreaks a greater incidence in infants and children than in adolescents. In the opposite, when incidences present high peaks followed by deep valleys (Figs. 3a and c and 7) it is observed at the outbreaks a greater incidence in adolescents than in infants and children. This correlation between dynamic behavior of incidences and the age distribution at outbreaks holds for the data obtained from epidemiological reports as well as for the results obtained from our model simulations.

Although this agreement between real and model data would be important to at least explore the major causes for pertussis resurgence in each state, it is necessary to remark at this point that the profiles and numerical estimates from epidemiological reports are subject to various factors that are difficult to determine, especially considering only notifications, such as the sensitivity of clinician suspicion, surveillance system or diagnostic methodology, the population background, etc.

Another aspect we want to stress is that in the case of contact transmission rates, we have mentioned different possible

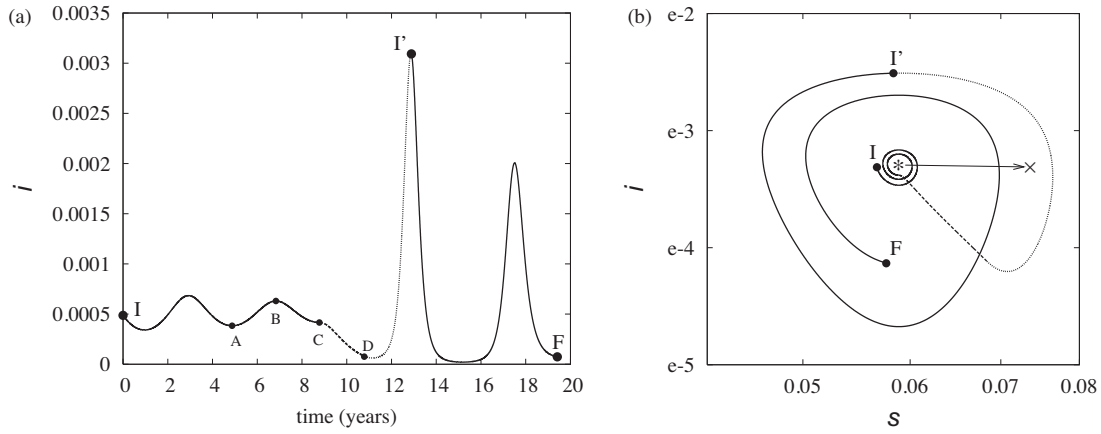

Fig. 8. Dynamic behavior of SIR model when the contact rate parameter β is changed. Panel (a): fraction of infected individuals as a function of time, $i(t)$. At point C, β was linearly reduced to 80% of its initial value over 2 years (dashed line) and then increased to the original value over the 2 following years (dotted line). From point I to C and I′ to F the system evolves with constant value of β (continuous line). The incidence (not shown) presents identical behavior to $i(t)$. Panel (b): fraction of infected vs. susceptible individuals for the system evolution described in Panel (a). The arrow indicates the shift of the stationary state of the system from $(s^*, i^*) = (0.0588, 0.00051)$ to $(s^X, i^X) = (0.0736, 0.00049)$ when β is reduced from 0.81 $1/d$ to 0.65 $1/d$.

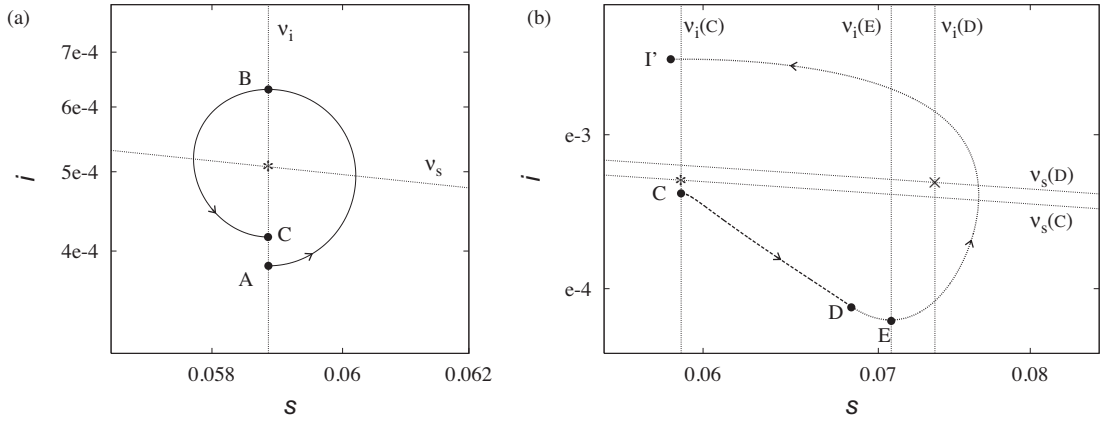

Fig. 9. Fraction of infected vs. susceptible individuals and nullclines ν_i and ν_s for part of the system evolution presented in Fig. 8. Panel (a): dynamic evolution of the system from point A to point C (Fig. 8a). Nullclines remain fixed in this period, as $\beta = 0.81\ 1/d$ = constant. The stationary point is located where nullclines intersect. Panel (b): dynamic evolution of the system from point C to point I′ (Fig. 8a). When β decreases (dashed line) nullcline ν_s shifts to the right and ν_i shifts upward. When β increases (dotted line) nullcline ν_s shifts to the left and ν_i shifts down.

underlying biological and social causes for a change in β_{ij}. Moreover, our statement about the appearance of pertactin deficient isolates is not the only cause that may trigger a decrease in β_{ij}. However, it is a cause that deserves to be fully explored given the spatial and temporal agreement in the detection of these isolates in the state of Washington in 2012 when the outbreak is observed.

Conclusions

In this work we presented results obtained with the age-structured deterministic model designed by us to study pertussis transmission disease. This model is useful to assess the impact of certain parameters that could be associated with the underlying causes of disease resurgence as are the reduction in VE with time and global changes in contagiousness as consequence, among others, to the pathogen evolution.

When these parameters were changed independently, we found that VE and β_{ij} changes affect the epidemiological trends of pertussis in regard to dynamic evolution of incidences and proportion of cases by age. Interestingly these changes were different: while reducing VE leads to a sustained increase in cases predominantly in infants and children, global changes in β_{ij} lead to large outbreaks with abrupt subsequent decline in cases. In the latter situation, pertussis is prevalent in adolescents. These results were reproduced in 18 different possible epidemiological scenarios indicating that the obtained results are robust and not a consequence of a particular choice of parameters.

More interestingly, we observed that the epidemiological trends predicted by the model when VE is reduced or when β_{ij} are changed, were similar to those reported by health systems in different regions, specifically in various states of US.

This agreement between the predicted trends and the reported data could have many explanations since neither the model could account for the whole complexity of pertussis, nor the notifications are a reflection of reality. However, the robustness of the results suggests some clues that deserve to be inspected as they may contribute to identify possible causes of the disease resurgence.

Beyond the ability of the model to shed light on the underlying determinants of pertussis epidemiology, the study presented here positions this model- and models in general- as a valuable tool in predicting the effects and assessing their impacts in the monitoring of infectious diseases.

Acknowledgments

This work was supported by Agencia Nacional de Promoción Científica y Tecnológica-ANPCyT, Comisión de Investigaciones Científicas de Buenos Aires-CICBA and Consejo Nacional de Investigaciones Científicas y Tecnológicas-CONICET (Argentina) grants to DFH and GF. GF, PB are members of the Scientific Career of CONICET. DFH is a member of the Scientific Career of CICBA. PP has fellowship from ANPCyT (grant 2010-0707).

Appendix.

The dynamic effect that takes place when effective contact rates are changed is not due to specific complexities of our age-structured epidemiological model, since it is already observed in the SIR model. In SIR model, the dynamics of the system can be drawn in the i–s plane because there are only two independent variables. This allows an easier understanding of the dynamic effects. We have considered a SIR model with vital dynamics, described by equations:

$$\begin{aligned}\frac{ds}{dt} &= -\beta is + \mu(1-p) - \mu s\\ \frac{di}{dt} &= \beta is - \gamma i - \mu i\\ \frac{dr}{dt} &= \gamma i + \mu p - \mu r\end{aligned} \tag{A.1}$$

where s, i and r are the fractions of susceptible, infected and recovered individuals respectively, β is the contact rate, γ is the recovery rate, μ is the death and birth rate and "p" is the fraction of population that is successfully immunized. For the parameters we have initially taken: $\gamma = 1/(21\text{days})$, $\beta = 17\gamma$, $\mu = 1/(50\text{years})$ and $p = 0.5$. With these values we obtained a period of oscillation of around 4 years, similar to that of the 9 class age-structured model used in this work prior to the consideration of the parameter changes. We give initial values to s and i ($r = 1 - s - i$), let the system evolve, and at a given time we change β in the same way as we did for β_{ij} before. The fraction of infected people as a function of time is shown in Fig. 8a from an initial time t_I to a final time t_F. The dynamic evolution of $i(t)$ shows the same behavior as Inc(t) in Fig. 3c. The dynamic trajectory in the i–s plane from I to F is presented in Fig. 8b. The oscillations of i with time observed in Fig. 8a between points I and C correspond to the orbits of decreasing amplitude around the stationary point (s^*, i^*) observed in Fig. 5b. This dynamic behavior of the SIR model around the attractor is well known and presented elsewhere (van den Driessche and Wu, 2008). When β parameter is decreased to 80% of its original value, the stationary state of the system is temporarily shifted to the point (s^X, i^X) as is indicated with an arrow in Fig. 8b. When β recovers its original value, the stationary state returns to (s^*, i^*) but the system is then at a new state I' far away from there. The system then describes large radius orbits that correspond to the high peaks with deep valleys in Fig. 8a.

To analyze the reason that drives the system to I', so far from the stationary state, we rewrite the Eq. (A.1) in the following way:

$$\begin{aligned}\frac{ds}{dt} &= -\beta s(i - i_n), \quad i_n = \frac{\mu(1-p)}{\beta s} - \frac{\mu}{\beta}\\ \frac{di}{dt} &= \beta i(s - s_n), \quad s_n = \frac{\gamma + \mu}{\beta}\end{aligned}$$

From these equations it is clear that s increases when $i < i_n$ and i increases when $s > s_n$. The nullclines: $\nu_s = \{(s, i), i = i_n\}$ and $\nu_i = \{(s, i), s = s_n\}$ contain sets of points where s and i are stationary respectively (Strogatz, 1994). In Fig. 9a we plot the trajectory of the system in the i–s plane from point A–C and the nullclines (which remain fixed in this period as β is constant). Point A is in nullcline ν_i so at that time i does not change and (as $i < i_n$) s increases. When s becomes greater than s_n, i begins to increase until it crosses again the nullcline ν_i at B. In this way the dynamics of the system may be easily understood from A to C. If β remained fixed, the system would continue towards (s^*, i^*), which is an attractor for this dynamical system. But from point C, β changes with time and so do the nullclines, as s_n and i_n depend on β. Fig. 9b shows the evolution of the system from C to I' and the nullclines for times corresponding to points C–E. At point C, $di/dt = 0$ and $ds/dt > 0$, if the nullcline ν_i were fixed, one would expect i to increase thereafter as was the case at point A because s would become greater than s_n. But when the system is at C, nullcline ν_i begins to move to the right quicker than s, so s becomes smaller than s_n and di/dt becomes negative. This explains why i decreases from C to D. The speed of the nullcline to the right depends on the rate of change of β, if $d\beta/dt$ were smaller, the effect would be less pronounced [see Fig. S4 in Suppl. Mat. for the effect of lowering $d\beta_{ij}/dt$ in the age-structured model]. From point D, i continues to decrease until nullcline ν_i (which is moving to the left) intersects the dynamic trajectory at the minimum of the curve in E (Fig. 9b). As $i \ll i_n$ at E, ds/dt is very high and the system reaches a high value of s while ν_i continues going back to the left. When s reaches its maximum, it is very apart from the nullcline ($s \gg s_n$) and di/dt is very high driving i to reach a very high value at I'. In this way, when the stationary state of the system has returned to its original value (s^*, i^*), the system is far away from it, at I'.

Appendix B. Supplementary data

Supplementary data associated with this article can be found, in the online version, at doi:10.1016/j.epidem.2014.04.001.

References

Advani, A., Gustafsson, L., Ahrén, C., Mooi, F.R., Hallander, H.O., 2011. Appearance of Fim3 and ptxP3-Bordetella pertussis strains, in two regions of Sweden with different vaccination programs. Vaccine 29 (18), 3438–3442, http://dx.doi.org/10.1016/j.vaccine.2011.02.070.

Alabama Department of Health, 2009. http://adph.org/Immunization/assets/2009PertussisCasesByAgeGroup.pdf (accessed 28.02.14).

Barkoff, A.M., Mertsola, J., Guillot, S., Guiso, N., Berbers, G., He, Q., 2012. Appearance of Bordetella pertussis strains not expressing the vaccine antigen pertactin in Finland. Clin. Vaccine Immunol. 19 (10), 1703–1704.

Bouchez, V., Brun, D., Cantinelli, T., Dore, G., Njamkepo, E., Guiso, N., 2009. First report and detailed characterization of *B. pertussis* isolates not expressing pertussis toxin or pertactin. Vaccine 27, 6034–6041.

CDC, Centers for Disease Control and Prevention. MMWR weekly report. http://www.cdc.gov/mmwr/mmwr_wk/wk_pvol.html (accessed 28.02.14).

de Melker, H.E., et al., 2006. The incidence of *Bordetella pertussis* infections estimated in the population from a combination of serological surveys. J. Infect. 53, 106–113.

DeBolt, C., Tasslimi, A., Bardi, J., Leader, B.T., Hiatt, B., Quin, X., Patel, M., Martin, S., Tondella, M.L., Cassiday, P., Faulkner, A., Messonnier, N.E., Clark, T.A., Meyer, S., 2012. Pertussis Epidemic, 61. MMWR CDC Surveill Summ., Washington, pp. 517–522.

Fabricius, G., Bergero, P.E., Ormazabal, M.E., Maltz, A.L., Hozbor, D.F., 2013. Modelling pertussis transmission to evaluate the effectiveness of an adolescent booster in Argentina. Epidemiol. Infect. 141, 718–734, http://dx.doi.org/10.1017/S0950268812001380.

Hegerle, N., Paris, A.S., Brun, D., Dore, G., Njamkepo, E., Guillot, S., Guiso, N., 2012. Evolution of French Bordetella pertussis and Bordetella parapertussis isolates: increase of Bordetellae not expressing pertactin. Clin. Microbiol. Infect. 18 (9), E340–E346, http://dx.doi.org/10.1111/j.1469-0691.2012.03925.x.

Hethcote, H.W., 1997. An age-structured model for pertussis transmission. Math. Biosci. 145, 89–136.

Klein, N.P., Bartlett, J., Rowhani-Rahbar, A., Fireman, B., Baxter, R., 2012. Waning protection after fifth dose of acellular pertussis vaccine in children. N. Engl. J. Med. 367, 1012–1019.

Klein, N.P., Bartlett, J., Fireman, B., Rowhani-Rahbar, A., Baxter, R., 2013. Comparative effectiveness of acellular versus whole-cell pertussis vaccines in teenagers. Pediatrics 131, 1716–1722.

Lam, C., Octavia, S., Bahrame, Z., Sintchenko, V., Gilbert, G.L., Lan, R., 2012. Selection and emergence of pertussis toxin promoter ptxP3 allele in the evolution of Bordetella pertussis. Infect. Genet. Evol. 12 (2), 492–495, http://dx.doi.org/10.1016/j.meegid.2012.01.001.

Luz, P.M., Codeço, C.T., Werneck, G.L., Struchiner, C.J., 2006. A modelling analysis of pertussis transmission and vaccination in Rio de Janeiro, Brazil. Epidemiol. Infect. 134, 850–862.
McCarthy, M., 2013. Acellular vaccines provided less protection during California pertussis outbreak. Br. Med. J. 346.
Misegades, L.K., Winter, K., Harriman, K., Talarico, J., Messonnier, N.E., Clark, T.A., Marti, S.W., 2012. Association of childhood Pertussis with receipt of 5 doses of Pertussis vaccine by time since last vaccine dose, California, 2010 Pertussis vaccine receipt and Pertussis infection. J. Am. Med. Assoc. 308, 2126–2132.
Montana Public Health and Human Services, 2012. http://www.dphhs.mt.gov/publichealth/immunization/documents/2012PertussisSummary.pdf (accessed 28.02.14).
Mooi, F.R., 2010. Bordetella pertussis and vaccination: the persistence of a genetically monomorphic pathogen. Infect. Genet. Evol. 10, 36–49.
Mooi, F.R., van Loo, I.H.I.H., van Gent, M., He, Q., Bart, M.J., Heuvelman, K.J., de Greeff, S.C., Diavatopoulos, D., Teunis, P., Nagelkerke, N., Mertsola, J., 2009. Bordetella pertussis strains with increased toxin production associated with pertussis resurgence. Emerg. Infect. Dis. 15 (8), 1206–1213, http://dx.doi.org/10.3201/eid1508.081511.
Ohio Department of Health, 2010. http://www.odh.ohio.gov/~/media/ODH/ASSETS/Files/bidstats/2010/10Age.ashx (accessed 28.02.14).
Otsuka, N., Han, H.J., Toyoizumi-Ajisaka, H., Nakamura, Y., Arakawa, Y., Shibayama, K., Kamachi, K., 2012. Prevalence and genetic characterization of pertactin-deficient Bordetella pertussis in Japan. PLoS ONE 7 (2), e31985, http://dx.doi.org/10.1371/journal.pone.0031985.
Pawloski, L.C., Queenan, A.M., Cassiday, P.K., Lynch, A.S., Harrison, M.J., Shang, W., Williams, M.M., Bowden, K.E., Burgos-Rivera, B., Qin, X., Messonnier, N., Tondella, M.L., 2014. Prevalence and molecular characterization of pertactin-deficient bordetella pertussis in the United States. Clin. Vaccine Immunol. 21 (2), 119–125, http://dx.doi.org/10.1128/CVI. 00717-13.
Petersen, R.F., Dalby, T., Dragsted, D.M., Mooi, F.R., Lambertsen, L., 2012. Temporal trends in Bordetella pertussis populations, Denmark, 1949–2010. Emerg. Infect. Dis. 18 (5), 767–774, http://dx.doi.org/10.3201/eid1805.110812.
Public Health England, 2013. Latest HPR – Laboratory-Confirmed Cases of Pertussis Reported to the Enhanced Pertussis Surveillance Programme: Q2/2013, Vol 7., pp. 34, http://www.hpa.org.uk/hpr/archives/2013/hpr14-1713.pdf, Published on: 23 August 2013 (accessed 30.08.13).
Rohani, P., Keeling, M.J., Grenfell, B.T., 2002. The interplay between determinism and stochasticity in childhood diseases. Am. Nat. 159, 469–481.
Schmidtke, A.J., Boney, K.O., Martin, S.W., Skoff, T.H., Tondella, M.L., Tatti, K.M., 2012. Population diversity among Bordetella pertussis isolates, United States, 1935–2009. Emerg. Infect. Dis. 18 (8), 1248–1255, http://dx.doi.org/10.3201/eid1808.120082.
Sheridan, S.L., Ware, R.S., Grimwood, K., Lambert, S.B., 2012. Number and order of whole cell pertussis vaccines in infancy and disease protection. J. Am. Med. Assoc. 308, 454–456.
Spokes, P.J., Quinn, H.E., McAnulty, J.M.J.M., 2010. Review of the 2008–2009 pertussis epidemic in NSW: notifications and hospitalisations. N. S. W. Public Health Bull. 21, 167–173.
Strogatz, S.H., 1994. Nonlinear Dynamics and Chaos. Perseus Books, U. S.
Texas Dep. of State Health Services, 2013a http://www.dshs.state.tx.us/idcu/disease/pertussis/statistics/incidence_mortality (accessed 28.02.14).
Texas Dep. of State Health Services, 2013b. Pertussis Cases in Texas by Age Group. http://www.dshs.state.tx.us/idcu/disease/pertussis/statistics (accessed 28.02.14).
van den Driessche, F.B.P., Wu, J., 2008. Mathematical Epidemiology. Springer, Germany.
van Gent, M., van Loo, I.H., Heuvelman, K.J., de Neeling, A.J., Teunis, P., Mooi, F.R., 2011. Studies on Prn variation in the mouse model and comparison with epidemiological data. PLoS ONE 6 (3), e18014, http://dx.doi.org/10.1371/journal.pone.0018014.
Warfel, J.M., Zimmerman, L.I., Merkel, T.J., 2014. Acellular pertussis vaccines protect against disease but fail to prevent infection and transmission in a nonhuman primate model. Proc. Natl. Acad. Sci. U. S. A. 111 (2), 787–792, http://dx.doi.org/10.1073/pnas.1314688110.
Washington State Department of Health, 2013. http://www.doh.wa.gov/Portals/1/Documents/Pubs/348-253-PertussisAnnualSummary.pdf (accessed 15.04.2013).
Winter, K., Harriman, K., Zipprich, J., Schechter, R., Talarico, J., Watt, J., Chavez, G., 2012. California pertussis epidemic, 2010. J. Pediatr. 161, 1091–1096.
Wisconsin Dep. of Health and Soc. Services, 2013. Number of reported confirmed and probable cases of pertussis, by age group and public health region. Pertussis Rep. Jan 15. http://www.dhs.wisconsin.gov/immunization/pdf/2012ASRpertussis.pdf (accessed 2.02.13).